Thermotropic Behavior of a Liquid Crystalline Polybibenzoate with an Asymmetric Oxymethylenic Spacer

Aránzazu Martínez-Gómez,* Antonio Bello, and Ernesto Pérez

Instituto de Ciencia y Tecnología de Polímeros (CSIC), Juan de la Cierva 3, 28006 Madrid, Spain

Received July 27, 2004; Revised Manuscript Received September 2, 2004

ABSTRACT: The thermotropic phase behavior of P3O4B, a polybibenzoate with an asymmetric oxymethylenic spacer, has been analyzed by DSC, real-time synchrotron X-ray diffraction, and optical microscopy. The results show that the following phases are found on cooling: isotropic melt, S_A mesophase, S_C mesophase, and three-dimensional crystal. The subsequent melting reveals the enantiotropic character of P3O4B since the inverse phase sequence is found. Additionally, a clear recrystallization process is observed on melting, prior to the crystal−S_C transition. The thermotropic properties of P3O4B are compared with those of its analogue polyester with an all-methylene spacer, poly(octamethylene *p*,*p*′-bibenzoate), P8MB, and other polybibenzoates with oxymethylenic spacers. Compared with P8MB, significantly lower transition temperatures are found for P3O4B due to the higher flexibility and asymmetry of the spacer. The lowering is especially important for the formation of the final crystal structure, so that the mesophase temperature window is considerably enlarged in P3O4B, allowing to observe the transition S_A to S_C. Moreover, the comparison of the thermotropic properties of P3O4B with those of other polybibenzoates with oxymethylenic spacers reveals that P3O4B is the only one able to crystallize at the usual cooling rates of the calorimeter.

Introduction

Main chain semiflexible polybibenzoates constructed by an alternative arrangement of biphenyl units as mesogenic groups and aliphatic spacers have been reported to exhibit thermotropic smectic phases.[1−8] The liquid crystalline behavior of these polymers hinges on the combination of the inherent anisotropic molecular interaction of the mesogenic units and their relative position in the macromolecular chain, which is dictated by the chemical structure and the even/odd character of the flexible aliphatic spacers connecting them.[1,2] Linear spacers with an even number of methylenic units show S_A mesophases, while for odd spacers the S_{CA} mesophase is found. A similar even−odd alternation of the smectic structures has been reported for the poly(ether ester)s derived from 4′-hydroxybiphenyl-4-carboxylic acid and alkanediols.[9] However, an opposite oscillation with the number of methylenic units is observed because, for the same alkanediol, the number of atoms connecting two successive biphenyl mesogens is lower by one unit in polyetheresters than in polyesters due to the lack of a carbonyl group. The even−odd effect has been explained as a consequence of the conformation of the alkylene spacer, which confines the spatial arrangement of the mesogenic groups in the smectic layers.[10,11]

It has been proved that the thermal properties of the mesophases and their transformation rate can be controlled with suitable changes in the structure of the flexible spacer.[6,8,11−14] A factor that can be managed is the stiffness of the molecular chains, governed by the number of conformations permitted to the chains, which can be modified by inserting bulky side groups and/or ether groups along the spacer. The information from previous works[8,11−13] indicates that as a result of substituting methylenic groups by ether linkages in the spacer, the thermal transitions of thermotropic polyesters are shifted to lower temperatures, the thermodynamic behavior becomes enantiotropic, and the rate of transformation of the mesophase into a more ordered phase is considerably decreased. Moreover, S_C mesophases have been reported for some oxymethylenic spacers[12] and methylenic spacers with methyl substitutents.[6,14] In recent works carried out in our laboratory, stable mesophases have been also obtained using asymmetric branched oxymethylenic spacers.[13,15] An odd−even effect on transition parameters and mesophase structure was also found. Therefore, the nature of the flexible spacer is very important for the thermotropic behavior of these polyesters.

Traditionally, the phase transitions in polymers (and materials, in general) were located by DSC experiments while the structural information about the phases involved is mainly obtained by X-ray diffraction. However, in recent years, both aspects (phase transitions and structural information) can be determined by real-time variable-temperature diffraction experiments using synchrotron radiation. The short acquisition times required for these synchrotron experiments make this technique particularly useful for the characterization of systems with a complicated phase behavior, as it happens in thermotropic liquid crystalline polymers where different phases are formed (and, particularly, in the present system). As will be show below, synchrotron experiments allow one to locate the phase transitions, to determine many aspects of the structure of the phases involved, and to obtain rather interesting information about the temperature variation of different structural parameters.

The aim of this work is the study of the liquid crystalline behavior of a new polybibenzoate containing an asymmetric oxymethylenic spacer derived from the ether−diol 4-(3-hydroxypropoxy)butan-1-ol, which has been synthesized by ring opening of oxetane with 1,4-butanediol in protonic conditions. The thermal behavior and mesophase structures of this polybibenzoate, named P3O4B, have been investigated by differential scanning

* Corresponding author. E-mail: icts319@ictp.csic.es.

10.1021/ma048458z CCC: $27.50
Published on Web 10/21/2004

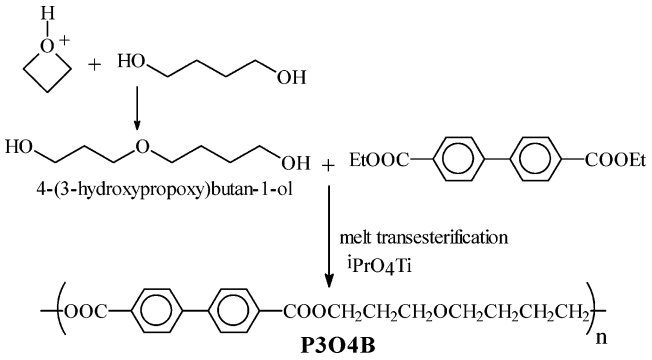

Figure 1. Synthesis of polybibenzoate P3O4B.

calorimetry, optical microscopy, and real-time X-ray diffraction experiments. Its thermotropic properties are compared with those found for other polybibenzoates described in the literature. As will be shown, a rather unique and interesting phase behavior is presented by P3O4B.

Experimental Section

Synthesis. Polymer P3O4B was obtained according to Figure 1. The details of the different steps are as follows.

Materials. Oxetane (Fluka) was purified by distillation from several sodium mirrors in a vacuum line, and 1,4-butanediol (Aldrich) was distilled at reduced pressure before use. Diethyl 1,1′-biphenyl-4,4′-dicarboxylate was synthesized as previously reported.[13] Titanium(IV) isopropoxide from Aldrich Co. was used as received.

Ether−Diol 4-(3-Hydroxypropoxy)butan-1-ol. The ether−diol used as flexible spacer was synthesized by the ring-opening reaction of oxetane with 1,4-butanediol initiated by sulfuric acid. A big excess of 1,4-butanediol was used, and oxetane was slowly added over the reaction mixture in order to keep a low instantaneous concentration of oxetane. Under these experimental conditions, the reaction is limited mainly to the first addition step.[15] The following procedure was applied: 20.11 g (0.34 mol) of oxetane was added dropwise to a solution of sulfuric acid (4.0 g, 0.04 mol) in 1,4-butanediol (113 g, 1.25 mol). This solution was degassed prior to the addition. The reaction mixture was stirred under vacuum at room temperature for 24 h. The mixture was poured into water, neutralized with aqueous sodium bicarbonate, and filtered. The product was extracted with chloroform and purified by consecutive distillations under vacuum. However, small amounts of higher oligomers (trimer) and/or unreacted 1,4-butanediol were always present in the distillated fractions. Then, trimethylsilyl groups were used to protect the hydroxyl functions, allowing us to purify the diol by flash chromatography in silica gel. The trimethylsilyl protecting group can be removed under mild conditions, for example by heating in aqueous alcohol under reflux.[16] The protection reaction was carried out by treatment with trimethylsilyl chloride−triethylamine: 11.7 g of impure glycol and 30 mL of triethylamine were dissolved in 200 mL of anhydrous THF. The mixture was vigorously stirred, and 25 mL of trimethylsilyl chloride were added dropwise at 0 °C. The formation of a white precipitate corresponding to Et_3NHCl is immediately observed. The mixture was stirred for 12 h at room temperature under a N_2 atmosphere. The white precipitate was filtered off and washed with THF. The filtrate was concentrated, and the protected diol was purified by flash chromatography (silica gel, hexane/ethyl acetate 95/5 as eluent). Yield 90%.

The chemical structure of the protected diol was checked by ^{1}H NMR in deuterated chloroform. ^{1}H NMR: $\delta = 0.08$ (s, 18H, $Si(CH_3)_3$), 1.57 (m, 4H, $OCH_2CH_2CH_2CH_2OSi(CH_3)_3$), 1.76 (q, 2H, $(CH_3)_3SiOCH_2CH_2CH_2O$), 3.40 (t, 2H, $OCH_2CH_2CH_2CH_2OSi(CH_3)_3$), 3.45 (t, 2H, $OCH_2CH_2CH_2CH_2OSi(CH_3)_3$), 3.57 (t, 2H, $(CH_3)_3SiOCH_2CH_2CH_2O$), 3.64 ppm (t, 2H, $(CH_3)_3SiOCH_2CH_2CH_2O$).

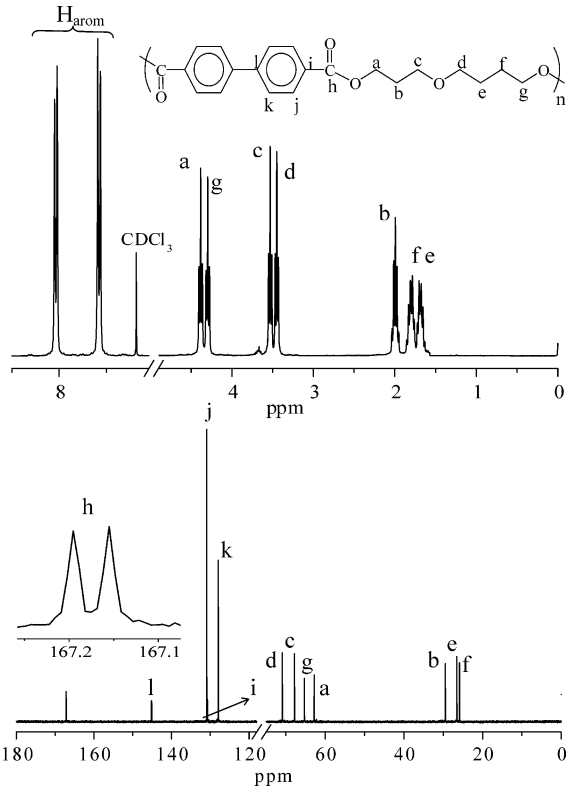

Figure 2. ^{1}H NMR and ^{13}C NMR spectra of P3O4B in deuterated chloroform at 40 °C.

The protecting trimethylsilyl ether groups were removed by stirring in a methanol−water mixture for 48 h under reflux. Methanol and water were eliminated, and the diol was distilled under vacuum. Its chemical structure was characterized by ^{1}H and ^{13}C NMR in deuterated chloroform. ^{1}H NMR ($CDCl_3$): $\delta = 1.62$ (m, 4H, $OCH_2CH_2CH_2CH_2OH$), 1.80 (q, 2H, $HOCH_2CH_2CH_2CH_2O$), 2.30 (s, 2H, O*H*), 3.46 (t, 2H, OCH_2), 3.60 (m, 4H, OCH_2 and CH_2OH), 3.74 ppm (t, 2H, CH_2OH). ^{13}C NMR ($CDCl_3$): $\delta = 26.9$ ($OCH_2CH_2CH_2CH_2OH$), 30.2 ($OCH_2CH_2CH_2CH_2OH$), 32.5 ($HOCH_2CH_2CH_2O$), 61.4 ($HOCH_2CH_2CH_2O$), 62.8 ($OCH_2CH_2CH_2CH_2OH$), 69.7 ($HOCH_2CH_2CH_2O$), 71.5 ppm ($OCH_2CH_2CH_2CH_2OH$).

Polymerization. The polyester P3O4B was prepared by melt transesterification of diethyl 1,1′-biphenyl-4,4′-dicarboxylate and 4-(3-hydroxypropoxy)butan-1-ol, using titanium(IV) isopropoxide as catalyst. The polymerization procedure was as follows: first, the diester (3.48 g, 11.7 mmol) and the diol (2.04 g, 13.8 mmol) were heated at 180−185 °C, then the catalyst was added, and the mixture was stirred under an inert atmosphere (N_2) for several hours. In a second step, polycondensation was carried out at higher temperature (220−250 °C) under reduced pressure (0.01 mmHg) for 4 h.

The polymer was purified by dissolving in hot chloroform and precipitating in excess methanol. The polymer was collected by filtration, washed with methanol, and dried in a vacuum. The recovered material was close to 90% of the theoretical yield.

The chemical structure of polymer P3O4B was characterized by means of NMR spectroscopy (see ^{1}H NMR and ^{13}C NMR spectra and signal assignments in Figure 2). The spectra do not show any unexpected signal. Because of the asymmetry of the flexible spacer, the ^{13}C NMR spectrum shows splitting of the resonance of the aromatic carbons and of the carbonyls (see amplification in Figure 2 for the carbonyls).

Size-exclusion chromatography data were obtained using a Waters 150C gel permeation chromatograph, equipped with two detectors: the conventional refractive index concentration detector and a viscometer Retrofit GPC 150R from Viscotek Co. The universal calibration was obtained from measurements in different polystyrene standards, using chloroform as

eluent at 25 °C. The peak molecular weight value obtained for P3O4B was M_p = 32 100, and the molecular weight averages were M_w = 31 400 and M_n = 12 100.

Liquid Crystalline Behavior. The thermal behavior of the polymer was studied by differential scanning calorimetric (DSC) experiments. DSC measurements were carried out with a Perkin-Elmer DSC7 calorimeter, provided with a cooling system. A scanning rate of 8 °C/min was used, and the sample weight was 10 mg.

The phase transitions and the symmetry of the phases involved at the thermal transitions were investigated by real-time X-ray diffraction experiments with synchrotron radiation. The short acquisition times required for the synchrotron experiments make this technique particularly useful for the characterization of liquid crystal systems where more than one mesophase are formed or where the mesophases present a short interval of existence. These experiments were performed at the polymer beamline at Hasylab (Desy, Hamburg). The beam was monochromatized (λ = 0.150 nm) by Bragg reflection through a germanium single crystal. Two linear position-sensitive detectors were used simultaneously, one of them fixed and covering the approximate 2θ range from 10° to 30° and the other being set at two different sample−detector positions (in the direction of the beam): 43 and 190 cm, respectively. The first position covers the approximate 2θ range from 1.1° to 8.8° (spacings from 8 to 1 nm) and the second from about 0.24° to 2.70° (spacings from about 35 to 3.2 nm). Therefore, wide-angle (WAXS), middle-angle (MAXS), and small-angle scattering (SAXS) data are collected in the two experimental setups: simultaneous WAXS/MAXS profiles are acquired in the first case and WAXS/SAXS in the second.

Film samples, of about 20 mg, were covered by aluminum foil to ensure homogeneous heating or cooling and placed in the temperature controller of the line under vacuum. Heating or cooling experiments were performed at a rate of 4 °C/min. The same temperature program was reproduced in the two setups, and the WAXS data were used to monitor the reproducibility of the results. The reproducibility was found to be well inside the inherent experimental resolution of the system.

The scattering patterns were collected in time frames of 30 s, so that we have a temperature resolution of 2 °C between frames. The calibrations of the spacings for the different detectors and positions were made as follows: the diffractions of a crystalline PET sample were used for the WAXS detector; a sample of silver behenate (giving a well-defined diffraction at a spacing of 5.838 nm and several orders) was used for the MAXS detector; and the different orders of the long spacing of rat-tail cornea (L = 65 nm) for the SAXS detector.

The polymer film for DSC and synchrotron measurements was prepared by molding the material in a Collin press above the melting temperature and then cooling to room temperature.

Fiber WAXS patterns were obtained at room temperature using a flat-plate camera attached to a Phillips 2 kW tube X-ray generator.

The mesophase textures were studied using a Carl Zeiss polarizing microscope equipped with a Linkam TMS92 hot stage.

Results and Discussion

The DSC curves of P3O4B, at 8 °C/min, are shown in Figure 3. Three exothermic peaks at 147 °C (ΔH = 17.2 J/g), 141 °C (ΔH = 4.1 J/g), and 52 °C (ΔH = 12.0 J/g) are observed on cooling from the isotropic melt. The first transition in the cooling shows a small undercooling and has an associated enthalpy of 1.47 kcal/mol and a change of entropy of 3.5 cal/(mol K). This low value implies a great conformational disorder in the phase that suggests the formation of a low-order smectic mesophase, as will be confirmed below.

In the heating curve, four endotherms at 108 °C (ΔH = 5.8 J/g), 127 °C (ΔH = 8.3 J/g), 143 (ΔH = 2.7 J/g), and 160 °C (ΔH = 17.0 J/g) appear.

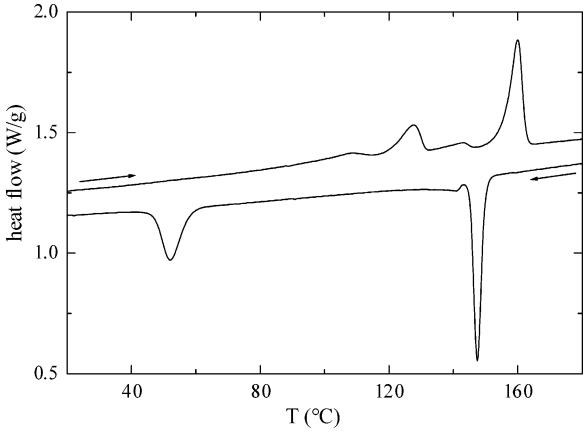

Figure 3. DSC curves of polymer P3O4B, at 8 °C/min, corresponding to the cooling from the isotropic melt and the subsequent heating.

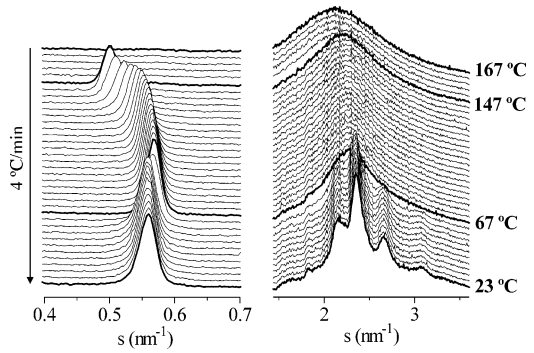

Figure 4. X-ray diffraction patterns in the MAXS (left side) and WAXS (right side) regions of P3O4B recorded during the cooling from the isotropic melt, at 4 °C/min. For clarity, only one of every two frames is plotted.

The nature of the phases was investigated by X-ray experiments and by the observation of birefringence textures with an optical microscope. The MAXS/WAXS synchrotron profiles in a cooling cycle at 4 °C/min are presented in Figure 4, and the most interesting results deduced from these profiles are shown in Figures 5 and 6 for the MAXS and WAXS regions, respectively. In this cooling experiment, it can be observed that at high temperatures (167 °C), when the polymer is an isotropic melt, only a broad halo, as a consequence of the averaged intermolecular distance, is observed in the WAXS region.

On lowering the temperature, at 149 °C the MAXS detector shows the appearance of a peak at around 0.502 nm^{-1} (1.99 nm) while the WAXS diffractograms show an amorphous-like halo. These features are characteristic of a low-order smectic phase. The MAXS diffraction is attributed to the regular piling of smectic layers, and the broad halo in the WAXS region indicates that the molecules are packing in an unstructured way into the layer. The spacing of 1.99 nm is close to the length of the full extended repeating unit of P3O4B (L = 2.24 nm), and this transition can be attributed to the formation of a S_A mesophase, characterized by an orthogonal localization of the molecules within the smectic layers.

The isotropic−smectic phase transition produces a slight change in the position of the WAXS halo. As it is shown in the upper part of Figure 6, a clear discontinuity is produced at about 148 °C, changing from 0.47 nm for the isotropic phase to 0.45 nm for the smectic one.

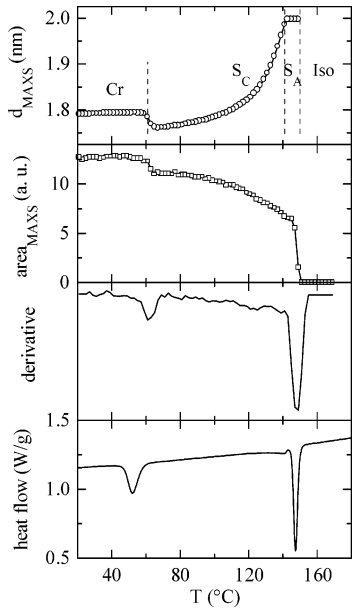

Figure 5. Variation of the position of the MAXS peak, total area, and its derivative as a function of temperature corresponding to P3O4B in the cooling experiment of Figure 4. The DSC cooling curve is presented in the lower part of the figure, for comparison.

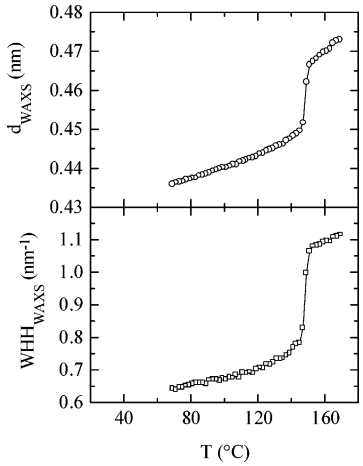

Figure 6. Variation of the position and width of the WAXS broad peak as a function of temperature for P3O4B on cooling from the isotropic melt.

After a few frames, the MAXS peak, coinciding with the small exotherm observed at 141 °C, begins to shift to lower spacings, from 1.99 nm to a final value of 1.76 nm at a temperature of 67 °C (see upper part of Figure 5). This reduction of the MAXS spacing can be interpreted as a tilting of molecules respect to the normal to the plane of the smectic layer. On the other hand, no change is observed in the WAXS diffractograms during the temperature interval in which d_{MAXS} shifting takes place, with the exception, as usual, of a slight linear decrease due to the thermal contraction. Therefore, we are dealing with a S_C mesophase.

The observations with the optical microscope under cross polarizers during the cooling reveal the formation of a fan-shaped texture. This texture is characteristic of smectic liquid crystals. The micrograph taken at 125 °C when cooling from the isotropic melt is shown in the left of Figure 7. No relevant changes were observed in the texture during the S_A–S_C transition.

According to the Landau–de Gennes theory, the second-order transition from S_A to S_C can be described by the continuous increase of the tilt angle, θ (taken as the order parameter of the transition), in such a way that the free energy can be expressed in terms of powers of the tilt angle.[2,17] In such case, and neglecting the higher powers of θ, i.e., for temperatures not far away from the temperature at which the tilt appears, T_c, the following equation is obtained:

$$\theta = k(T_c - T)^{0.5} \quad (1)$$

where k is a constant. The tilt angle (θ) can be estimated using the expression

$$\cos\theta = d_\theta/d_0 \quad (2)$$

where d_θ is the smectic spacing of S_C mesophase at different temperatures, and consequently at different tilt angles, and d_0 is the smectic spacing for a tilt angle equal to zero (S_A mesophase). Considering that d_0 is 1.99 nm for P3O4B, the variation with temperature of tilt angle has been displayed in Figure 8. It can be seen that in a certain interval the data are fitted rather well to a parabolic function of the type of eq 1, with $k = 6$ and $T_c = 141.5$ °C. As expected, the range of validity of eq 1 is restricted to temperatures not very much below T_c.

Continuing with the analysis of the synchrotron cooling experiment, it is observed that, by further decreasing the temperature below 67 °C, P3O4B undergoes a third transformation (thermal transition at 52 °C in the DSC measurements) detected by a small shift of the MAXS diffraction from 1.76 to 1.79 nm and the development of four sharp diffractions in the WAXS region (d = 0.463, 0.425, 0.376, and 0.325 nm), which suggest the formation of a phase with long-range positional order of the molecules within the layers: most probably a three-dimensional crystal. On the other

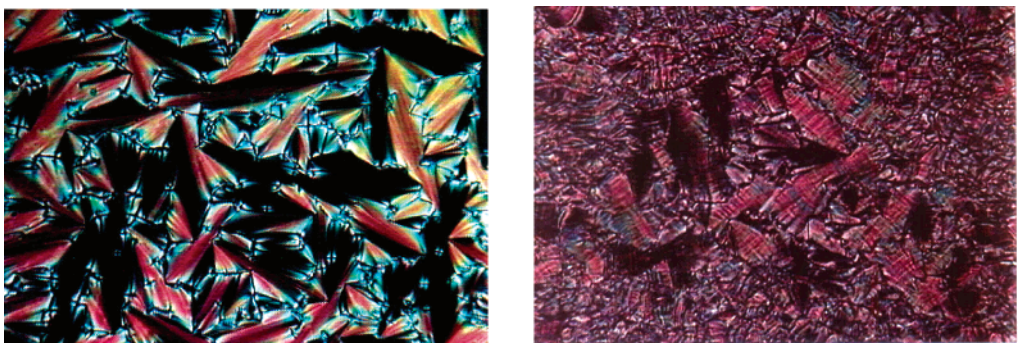

Figure 7. Optical polarized micrographs of P3O4B taken at 125 °C (left) and 20 °C (right) during a cooling experiment at 0.1 °C/min.

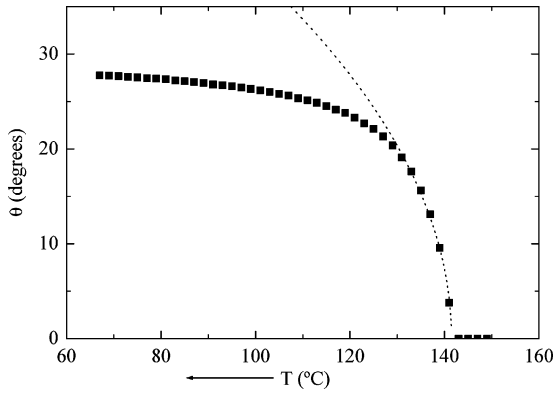

Figure 8. Temperature dependence of the tilt angle in the S_C mesophase of P3O4B. The dashed line correspond to the fitting to eq 1, with the parameters indicated in the text.

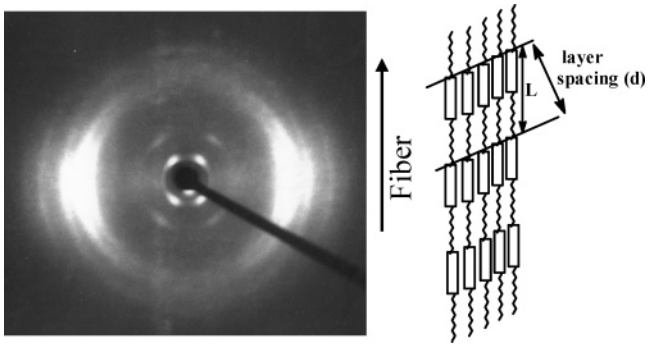

Figure 9. X-ray photograph at room temperature for a fiber of P3O4B obtained by uniaxial stretching.

hand, the optical polarizing experiments reveal the occurrence of concentric arcs in the smectic fans (see micrograph at the right of Figure 7). In liquid crystal substances which possess a S_A mesophase, it is very common to observe striated fan-shaped textures for their highly ordered phases.[18]

Comparing the MAXS spacing $d = 1.79$ nm with the spacing of the S_A mesophase ($d = 1.99$ nm), it seems that the ordered phase is an inclined structure. This has been confirmed by X-ray diffraction of an oriented sample. Figure 9 shows the diffraction pattern recorded at room temperature. The inner reflections attributed to the spacing between layers (two orders are observed) appear as four symmetric spots displaced from the meridional (direction of the macromolecular axis), indicating that the repeating unit (L) is tilted in relation to the layers. The tilt angle can be directly measured from the photograph, finding a value of 29°. This value is similar to that deduced using eq 2. The outer diffractions corresponding to the lateral arrangements of the molecules in the layers appear with the maximum of intensity on the equatorial plane. This fact indicates that the mesogenic groups lie parallel to the fiber axis. Considering all these results, the following phase sequence can be proposed for P3O4B in the cooling from the isotropic melt: I−S_A−S_C−Cr.

Additional information is deduced from the results presented in Figures 5 and 6. The upper part of Figure 5 shows the variation with temperature of the MAXS peak spacing. The first interesting feature is that in the temperature region where a mesophase S_A is presumably formed the temperature coefficient seems to be negative. (Only a few points are available, but this feature will be confirmed by the results of the subsequent melting experiment; see below.) A negative temperature coefficient of the mesophase has been also found in other similar polmers.[19,20] The interpretation is that the regular thermal contraction on cooling is counterbalanced by gauche−trans conformational transitions in the spacer.[11]

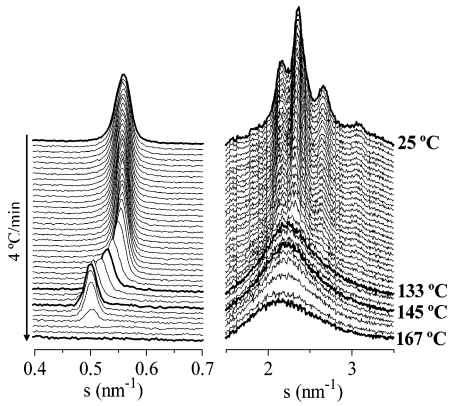

Figure 10. X-ray diffraction patterns in the MAXS (left side) and WAXS (right side) regions of P3O4B recorded during the heating at 4 °C/min. For clarity, only one of every two frames is plotted.

The variation with temperature of the area of the MAXS peak is also shown in Figure 5. It reflects rather clearly the different phase transition, in such a way that its derivative presents several peaks located at temperatures rather close to the DSC transitions, especially when considering the different cooling rates in the two kinds of experiments.

Regarding the WAXS results, presented in Figure 6, the variation of the spacing corresponding to the maximum of the amorphous-like wide peak is seen in the upper part of this figure. As commented above, an amorphous-like peak is observed in the isotropic melt, in the S_A and in the S_C mesophases, with a clear discontinuity when passing from the isotropic to the S_A phase. This discontinuity is observed in both the spacing and the width of the peak, as seen in Figure 6. On the contrary, a rather small (if any) change is observed on passing from the S_A to the S_C phase.

From the width of the WAXS wide peak and a simple application of the Scherrer equation,[21] it can be deduced that the correlation length, which is only of the order of 0.9 nm in the isotropic melt, increases significantly to a value of around 1.3 nm when the S_A mesophase is formed.

In the subsequent heating cycle (Figure 10), the polymer exhibits an enantiotropic behavior showing, approximately, the inverse phase sequence: Cr−S_C−S_A−I. The MAXS diffraction remains at around the same position until a temperature of about 111 °C, when the peak loses intensity, becomes wider, and begins to shift to higher spacings, from a value of 1.80 nm to the final value of 1.99 nm of the S_A mesophase at a temperature of 145 °C (see upper part of Figure 11). In the WAXS region, it can be observed that the four diffraction peaks of the Cr phase have completely disappeared at 133 °C (see Figure 10). Thus, the melting of Cr to give the S_C mesophase can be associated with the second endotherm detected in the DSC curve (127 °C). The transition S_C−S_A takes place in the interval 133−145 °C, when the calorimetric experiment shows that a small enthalpic change is produced (weak endotherm at 143 °C). Finally, the isotropization of the S_A mesophase is attained at 159 °C (fourth transition in

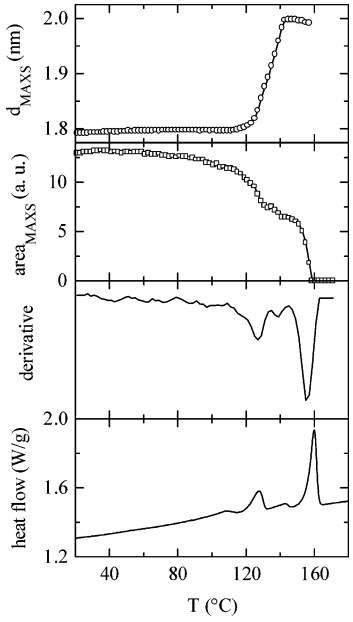

Figure 11. Variation of the position of the MAXS peak, total area and its derivative as a function of temperature corresponding to P3O4B in the heating experiment of Figure 10. The DSC heating curve is presented in the lower part of the figure, for comparison.

the DSC heating curve): the MAXS peak has disappeared, and an amorphous halo is observed in the WAXS region.

The detailed analysis of the synchrotron profiles in the melting experiment is presented in Figure 11. The upper part of this figure shows the variation of the MAXS spacing. Above 140 °C, where the S_A is formed, the temperature coefficient is negative, similarly to the cooling experiment as commented above. But now the temperature window where this mesophase is observed is slightly higher than in the cooling experiment, and the negative coefficient is more clearly ascertained.

The variation of the area of the MAXS peak is shown also in Figure 11, and its derivative presents rather similar peaks than the DSC experiment.

Only the first DSC transition, observed at around 108 °C, is not clearly observed in any of these MAXS results. Moreover, no significant changes in the WAXS profiles are observed, so that it seems that this transition should correspond to a recrystallization−melt phenomena. This has been analyzed by small-angle scattering (simultaneously with the wide-angle scattering, which has been used to test the reproducibility of the phase transitions in relation to the MAXS−WAXS experiments). Figure 12 shows the Lorentz-corrected profiles corresponding to a melting experiment. A rather weak long spacing, centered at around 20 nm, is observed at room temperature. On heating, the intensity of this long spacing increases, and it begins to move to higher spacings above 83 °C, with a maximum intensity at 107 °C. After that, its intensity decreases, disappearing completely at around 125 °C. The interpretation is, therefore, that the crystal structure formed during cooling P3O4B experiences a recrystallization process coinciding with the first DSC peak, and the long spacing is more clearly observed. However, when the S_C mesophase is formed, no long spacing is seen (at least inside the detector's window). No long spacing is observed either when the S_A mesophase is formed and obviously after isotropization.

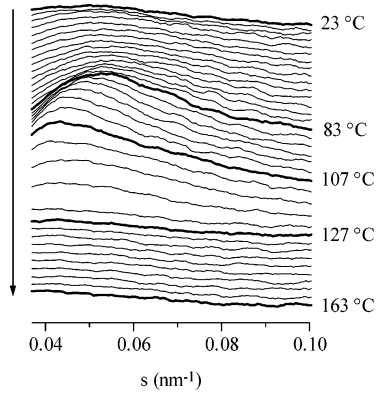

Figure 12. Lorentz-corrected SAXS profiles of P3O4B in a heating experiment at 4 °C/min.

Table 1. Transition Temperatures, Thermodynamic Parameters, and Smectic Spacing of Polybibenzoates P8MB and P3O4B

	P8MB[12,22]	P3O4B
phase sequence[a]	I 168 S_A 142 Cr	I 147 S_A S_C 52 Cr
T_m[b] (°C)	202[c]	127
ΔH_m (kcal mol^{-1})	3.9[c]	0.7
ΔS_m (cal mol^{-1} K^{-1})	8.2[c]	1.7
T_i[d] (°C)	196	160
ΔH_i (kcal mol^{-1})	2.30	1.4
ΔS_i (cal mol^{-1} K^{-1})	4.9	3.3
d[e] (nm)	2.06	1.99
L[f] (nm)	2.27	2.25

[a] On cooling from the isotropic melt. Transition temperatures in °C. [b] Melting temperature of the crystal phase. [c] Monotropic transition. [d] Isotropization temperature. [e] Layer spacing of the S_A mesophase. [f] Calculated length of the repeating unit assuming all-trans conformation.

It is of interest to compare the thermotropic properties of P3O4B with those of poly(octamethylene *p*,*p*′-bibenzoate) (P8MB), the analogue polyester with an all-methylene spacer. The transition temperatures and thermodynamic parameters are collected in Table 1. For both polymers the first phase formed on cooling the isotropic melt is a S_A mesophase. On further cooling, the mesophase is transformed into a more ordered phase, that is tilted for P3O4B. Moreover, in the case of P3O4B this transformation takes place through a S_C mesophase. The layer spacing of the S_A mesophase of P3O4B is somewhat smaller (0.07 nm) than that for P8MB. Similar reductions in the distance between smectic layers have been found for other oxymethylenic polybibenzoates.[11]

Regarding the transition temperatures, it is observed that they are considerably lower for P3O4B, especially the transition corresponding to the formation of the ordered structure, which amplifies the mesophase temperature region. This decreasing of the thermal transitions of P3O4B can be explained by considering its higher polymer chain flexibility, due to the presence of oxygen atoms in the spacer, and its less regular polymer structure. The structural irregularity is caused by the different sequences of the asymmetric ether−diol along the polymer backbone.

There is an important difference between P3O4B and P8MB. As was shown before,[22] the crystal of P8MB melts directly into the isotropic melt (monotropic behavior), and the mesophase is not detected on heating the polymer. The mesophase, however, can be observed on cooling from the melt prior to its transformation into the crystal. On the contrary, the results of this work

Table 2. Thermal Transitions and Phase Sequence of Polybibenzoates (PhPhCOOROOC)$_n$ with Oxymethylenic Spacers

polymer	spacer R	n^a	phase sequence[b]
PDEB[23]	$(CH_2)_2O(CH_2)_2$	5	I 184 S_{CA}
PETB[13]	$(CH_2)_3O(CH_2)_2$	6	I 178 S_A S_C
PDTMB[1,11]	$(CH_2)_3O(CH_2)_3$	7	I 154 S_{CA}
P3O4B	$(CH_2)_3O(CH_2)_4$	8	I 147 S_A S_C 52 Cr
PTEB[12]	$(CH_2)_2O(CH_2)_2O(CH_2)_2$	8	I 85 S_A S_C
PDETB[13]	$(CH_2)_3O(CH_2)_2O(CH_2)_2$	9	I 82 S_{CA}

[a] Sum of CH_2 and O groups in the spacer. [b] On cooling from the isotropic melt. Transition temperatures in °C.

show that P3O4B presents an enantiotropic behavior on heating since the ordered structure is transformed into the mesophase prior to its isotropization.

The polymer P3O4B can also be compared with other semiflexible polybibenzoates with oxymethylenic spacers that have been synthesized and analyzed previously in our laboratory (see Table 2). The following observations can be pointed out: (a) As is expected, the temperature of the isotropic−mesophase transition decreases as the spacer length increases. The lowering is higher in the case of polymers with two oxygen atoms in the spacer (PTEB and PDETB). (b) The even−odd effect described for the methylenic series is also found for this oxymethylenic series. The polymers with an even number of units in the spacer (PETB, P3O4B, and PTEB) exhibit a S_A mesophase, and the polymers with odd spacers (PDEB, PDTMB, and PDETB) form a S_{CA} mesophase. (c) For all the even polymers, the S_A mesophase is transformed into a tilted S_C mesophase. (d) There is, however, a distinctive feature for P3O4B: from all the polymers in Table 2, it is the only one where the crystal is formed at the usual rates of the calorimeter.

Conclusions

A rather interesting phase behavior has been found for P3O4B, a polybibenzoate with an asymmetric oxymethylenic spacer. The corresponding analysis by DSC, real-time synchrotron X-ray diffraction, and optical microscopy shows that, on cooling, the following phases are found: isotropic melt, S_A mesophase, S_C mesophase, and three-dimensional crystal. The subsequent melting reveals the enantiotropic character of P3O4B, since the reverse phase transitions are observed. Additionally, a clear recrystallization process is observed on melting, prior to the crystal−S_C transition.

Comparing the phase behavior of P3O4B with that of poly(octamethylene *p*,*p*′-bibenzoate), the analogue polybibenzoate with an all-methylene spacer, significantly lower transition temperatures are found for P3O4B due to the higher flexibility and asymmetry of the spacer. The lowering is especially important for the formation of the final crystal structure, so that the mesophase temperature window is considerably enlarged in P3O4B, allowing to observe the transition S_A to S_C.

Moreover, the comparison of the thermotropic properties of P3O4B with those of other polybibenzoates with oxymethylenic spacers reveals that P3O4B is the only one able to crystallize at the usual cooling rates of the calorimeter. From this comparative study it can also be concluded that this oxymethylenic series shows similar trends to that observed for the methylenic series: the temperature of the isotropic−mesophase transition decreases as the spacer length increases, and a S_A/S_{CA} oscillation with the even/odd character of the spacer is observed. However, for all the even polymers, the S_A mesophase is transformed into a S_C mesophase.

Acknowledgment. We acknowledge the financial support of MCYT, Project No MAT2001-1731. The synchrotron work was supported by the Contract HPRI-CT-1999-00040/2001-00140 of the European Community. We thank the collaboration of the Hasylab personnel.

References and Notes

(1) Pérez, E.; Pereña, J. M.; Benavente, R.; Bello, A. In *Handbook of Engineering Polymeric Materials*; Cheremisinoff, N. P., Ed.; Marcel Dekker: New York, 1997; p 383.
(2) Watanabe, J.; Hayashi, M.; Nakata, Y.; Niori, T.; Tokita, M. *Prog. Polym. Sci.* **1997**, *22*, 1053.
(3) Meurisse, P.; Nöel, C.; Monnerie, L.; Fayolle, B. *Br. Polym. J.* **1981**, *13*, 55.
(4) Krigbaum, W. R.; Asrar, J.; Toriumi, H.; Ciferri, A.; Preston, J. *J. Polym. Sci., Polym. Lett. Ed.* **1982**, *20*, 109.
(5) Watanabe, J.; Hayashi, M. *Macromolecules* **1989**, *22*, 4083.
(6) Pérez, E.; del Campo, A.; Bello, A.; Benavente, R. *Macromolecules* **2000**, *33*, 3023.
(7) Pérez, E.; Bello, A.; Marugán, M. M.; Pereña, J. M. *Polym. Commun.* **1990**, *31*, 386.
(8) Bello, A.; Pérez, E.; Marugán, M. M.; Pereña, J. M. *Macromolecules* **1990**, *23*, 905.
(9) Nakata, Y.; Watanabe, J. *J. Mater. Chem.* **1994**, *4*, 1699.
(10) Abe, A. *Macromolecules* **1984**, *17*, 2280.
(11) Bello, A.; Riande, E.; Pérez, E.; Marugán, M. M.; Pereña, J. M. *Macromolecules* **1993**, *26*, 1073.
(12) Pérez, E.; Riande, E.; Bello, A.; Benavente, R.; Pereña, J. M. *Macromolecules* **1992**, *25*, 605.
(13) Bello, P.; Bello, A.; Riande, E.; Heaton, N. J. *Macromolecules* **2001**, *34*, 181.
(14) Watanabe, J.; Hayashi, M.; Kinoshita, S.; Niori, T. *Polym. J.* **1992**, *24*, 597.
(15) Martínez-Gómez, A.; Bello, A.; Pérez, E. Submitted to *J. Polym. Sci., Part A: Polym. Chem.*
(16) Omie, J. F. W. Mc. *Protective Groups in Organic Chemistry*; Plenum Press: New York, 1973; p 103.
(17) Lagerwall, S. T. *Ferroelectric and Antiferroelectric Liquid Crystal*; Wiley-VCH: New York, 1999; p 115.
(18) Demus, D.; Richter, L. *Textures of Liquid Crystals*, 2nd ed.; VEB Deutscher Verlag für Grundstoffindustries: Leipzig, 1980.
(19) Pérez, E.; Todorova, G.; Krasteva, M.; Pereña, J. M.; Bello, A.; Marugán, M. M.; Shlouf, M. *Macromol. Chem. Phys.* **2003**, *204*, 1791.
(20) Todorova, G. K.; Krasteva, M. N.; Pérez, E.; Pereña, J. M.; Bello, A. *Macromolecules* **2004**, *37*, 118.
(21) Alexander, L. E. *X-ray Diffraction Methods in Polymer Science*; Wiley: New York, 1969.
(22) Pérez, E.; Zhen, Z.; Bello, A.; Benavente, R.; Pereña, J. M. *Polymer* **1994**, *35*, 4794.
(23) Pérez, E.; Benavente, R.; Cerrada, M. L.; Bello, A.; Pereña, J. M. *Macromol. Chem. Phys.* **2003**, *204*, 2155.

MA048458Z